Journal of Molecular Catalysis A: Chemical 320 (2010) 72–78

Contents lists available at ScienceDirect

Journal of Molecular Catalysis A: Chemical

journal homepage: www.elsevier.com/locate/molcata

Efficient catalytic oxidation of tetraethylated rhodamine over ordered mesoporous manganese oxide

Songmei Sun, Wenzhong Wang*, Meng Shang, Jia Ren, Ling Zhang

State Key Laboratory of High Performance Ceramics and Superfine Microstructure, Shanghai Institute of Ceramics, Chinese Academy of Sciences, 1295 Dingxi Road, Shanghai 200050, PR China

ARTICLE INFO

Article history:
Received 5 November 2009
Received in revised form
28 December 2009
Accepted 8 January 2010
Available online 15 January 2010

Keywords:
Manganese oxide
Catalysis
RhB
Decolorization
Mineralization

ABSTRACT

Ordered mesoporous manganese oxide (m-MnO_x) which consists of catalytic active MnO_2 and Mn_2O_3 phases has been successfully synthesized by a simple template casting method. The as-prepared m-MnO_x sample exhibited excellent catalytic activity on the degradation of tetraethylated rhodamine (RhB) dye. The degradation efficiency was found greatly influenced by the catalyst concentration, the reaction temperature and the pH value of the reaction system. The decrease of chemical oxygen demand (COD) value was also observed along with the decolorization indicating the mineralization of the dye.

1. Introduction

Synthetic dyes are extensively used today in not only the traditional textile and dyeing industries but also in new areas such as food, pharmaceutical, cosmetics, imaging biological samples, liquid crystals, lasers, solar cells, as well as optical data discs and computer industries [1]. These dyes being discharged into water bodies create severe environmental pollution problems by releasing toxic and potential carcinogenic substances for aquatic life as well as humans. Therefore, an effective treatment is environmentally important for the dye-containing effluents before they are discharged. Although the conventional physical processes such as precipitation, adsorption, air stripping, flocculation, reverse osmosis and ultrafiltration can be used for color removal from dye effluents [2–5], these techniques are non-destructive and giving rise to new type of pollution which needs further treatment [6–8]. Other conventional treatments based on biological process are destructive for dyes but usually ineffective because high molecular weight compounds are not easily degraded by bacteria [9].

Recent studies for dye removal from water have led to the development of catalytic oxidation process [10–12]. These processes involve chemical, photochemical or electrochemical techniques to bring about efficient chemical degradation of organic pollutants. Among the various catalysts used, manganese oxides have received great attention since they contain various types of labile oxygen, which are necessary to complete a catalytic cycle. Besides the catalytic oxidation of organic dyes [13–15], manganese oxides have other widely applications as catalyst, e.g., the decomposition of ozone [16,17] and H_2O_2 [18,19], the oxidation of carbon monoxide [20,21], the low-temperature selective catalytic reduction of NO with ammonia [22–24] and the catalytic oxidation of other organic compounds [25–27], etc. As is well known, the catalytic performance is significantly influenced by the surface area that directly determines the number of active sites [28,29]. Mesoporous manganese oxides with high surface area are very attractive. Especially, ordered mesoporous structures may exhibit much enhanced catalytic activity with continuous pore channels which facilitate the transfer of reactant molecules.

The dye under consideration is RhB. It is widely used in textiles, leathers and food stuffs with high water solubility. The objective of this study was to investigate the catalytic oxidation of RhB by mesoporous manganese oxides. The as-prepared mesoporous sample exhibits much higher catalytic activity than nonporous sample under the same conditions. The extent of dye decomposition was monitored using UV–vis spectroscopic techniques. The effects of the key operating variables, such as catalyst concentration, pH of the reaction solution, and reaction temperature on the rate of RhB decomposition were studied. The decrease of chemical oxygen demand (COD) value was also observed in the present study which further

* Corresponding author. Tel.: +86 21 5241 5295; fax: +86 21 5241 3122.
E-mail address: wzwang@mail.sic.ac.cn (W. Wang).

1381-1169/$ – see front matter © 2010 Elsevier B.V. All rights reserved.
doi:10.1016/j.molcata.2010.01.006

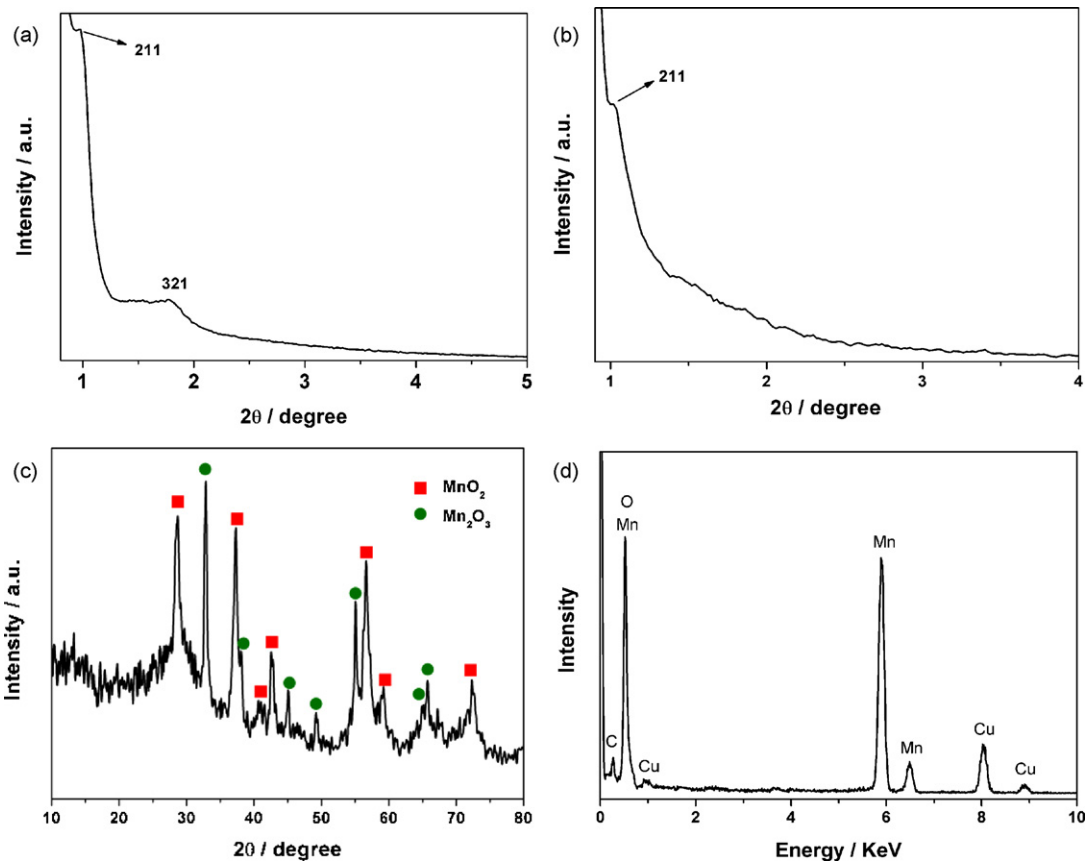

Fig. 1. Small-angle XRD patterns of (a) mesoporous cubic KIT-6 silica and (b) the as-prepared m-MnO_x sample (silica-free), (c) wide-angle XRD pattern of the as-prepared m-MnO_x sample (silica-free), and (d) EDS result of the as-prepared m-MnO_x sample.

proved the mineralization of the RhB dye by the m-MnO_x sample.

2. Experimental

2.1. Sample preparation

Mesoporous silica with cubic Ia3d symmetry (KIT-6) was prepared according to the reference using tri-block copolymer Pluronic P123 (EO20PO70EO20) as template in an acidic aqueous solution [30]. Typically, 4 g of P123 was dissolved in 146.6 g of distilled H_2O and 6.6 mL of concentrated HCl (35%). The mixture was stirred for several hours at 35 °C till a homogeneous solution was formed. Then 4 g of n-butanol was added under stirring. 9 mL of tetraethyl orthosilicate (TEOS) was finally added and stirred for 24 h at the same temperature. The mixture was heated at 100 °C for 24 h under static conditions for the hydrothermal treatment followed by filtration, washing, drying at 60 °C in air, and calcination at 550 °C for 5 h.

Ordered mesoporous MnO_x was prepared by a hard template replicating technique. Typically, 0.5 g of mesoporous KIT-6 was dispersed in 20 mL of *n*-hexane. After stirring at room temperature for 5 h, 0.4 mL of 50% $Mn(NO_3)_2$ solution and 0.1 mL of deionized water were added under stirring. After the mixture was evaporated gradually, the samples were calcined at 400 °C for 3 h to give a decomposed product of manganese oxides inside the silica template. The silica template was removed by 2 M NaOH solution under stirring. After washing with enough distilled water and drying at room temperature, the mesoporous MnO_x sample named as m-MnO_x was obtained. For comparison, the manganese oxide without using template was also obtained by decomposing $Mn(NO_3)_2$ directly and was named as nm-MnO_x.

2.2. Characterization

The purity and the crystallinity of the as-prepared samples were characterized by powder X-ray diffraction (XRD) on a Japan Rigaku Rotaflex diffractometer using Cu Kα radiation while the voltage and the electric current were held at 40 kV and 100 mA. The scanning electron microscope (SEM) characterizations were performed on a JEOL JSM-6700F field emission scanning electron microscope. The transmission electron microscope (TEM) analyses were per-

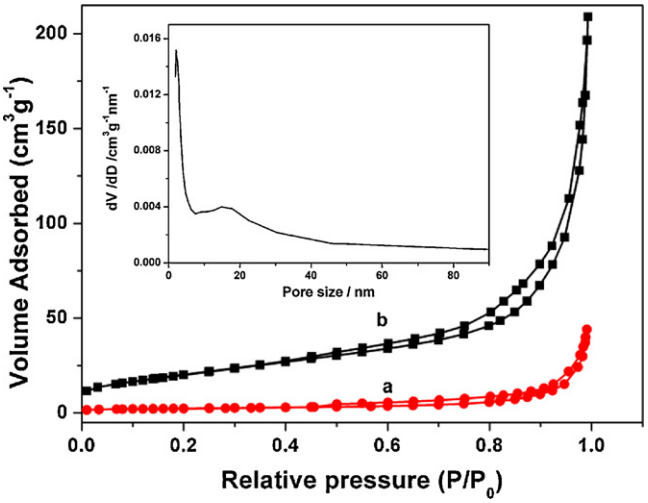

Fig. 2. Nitrogen sorption isotherms of nm-MnO_x (a) and m-MnO_x (b). Inset: the corresponding pore size distribution of the m-MnO_x sample.

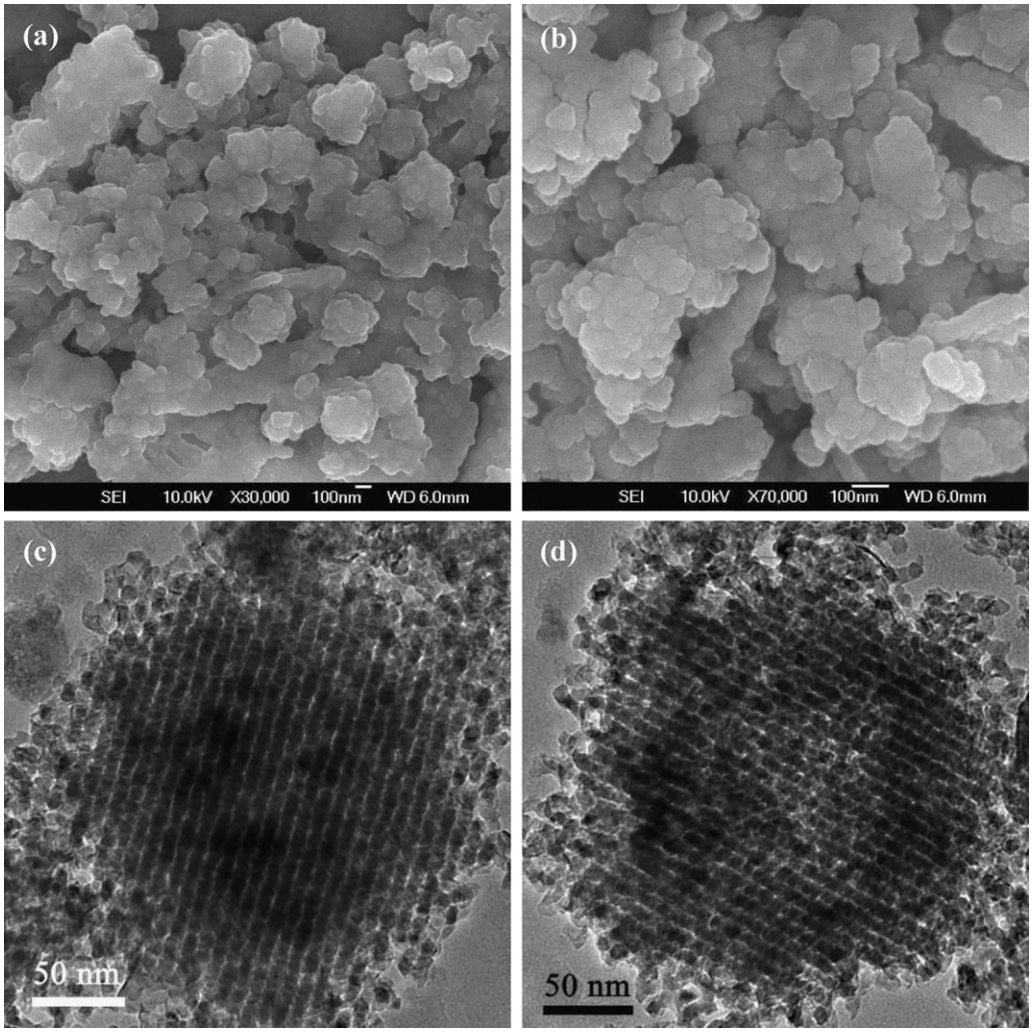

Fig. 3. SEM images (a and b) and TEM images (c and d) of the as-prepared m-MnO_x sample.

formed by a JEOL JEM-2100F field emission electron microscope. Energy-dispersive X-ray spectrum (EDS) was collected from an attached Oxford Link ISIS energy-dispersive spectrometer. The N_2 sorption measurement was performed using Micromeritics Tristar 3000 at −196 °C. The specific surface area and the pore size distribution were calculated using the Brunauer–Emmett–Teller (BET) and Barrett–Joyner–Halenda (BJH) methods, respectively.

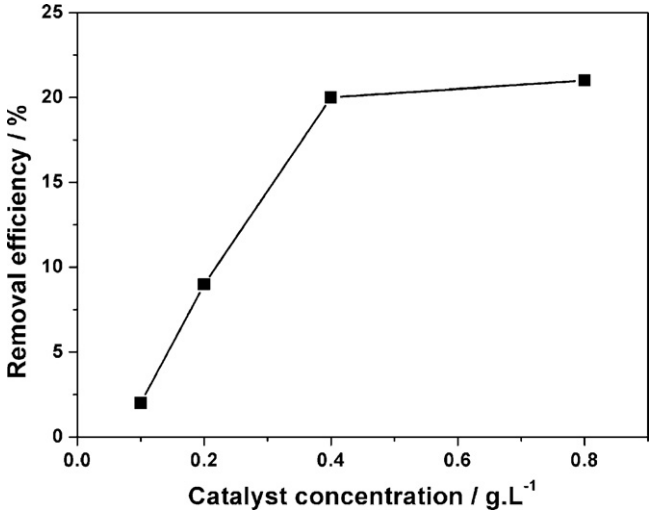

Fig. 4. Effect of catalyst concentration on decolorization efficiency of RhB (RhB concentration: 10^{-4} M, temperature 30 °C, pH 2.3).

2.3. Catalytic test

The catalytic degradation of RhB was carried out using a bath-type reactor under atmospheric condition. In a typical reaction run, a 100 mL of 10^{-4} mol/L RhB solution, previously adjusted to a fixed pH value with diluted HNO_3, was added to a 250-mL glass flask containing a certain amount of MnO_x catalyst. The suspensions were then heated to the reaction temperature (30–100 °C) under vigorous magnetic stirring. At every interval of few minutes, a 4 mL of suspension was sampled and centrifuged to remove the catalyst particles. Then, the adsorption UV–vis spectrum of the centrifugated solution was recorded using a Hitachi U-3010 UV-vis spectrophotometer. COD was estimated using the $K_2Cr_2O_7$ oxidation method.

3. Results and discussion

3.1. Characterization of the mesoporous manganese oxide sample

The low-angle XRD pattern of KIT-6 template in Fig. 1a shows a highly ordered cubic (*Ia*3*d*) mesostructure with a_0 = 22.2 nm. The XRD pattern of the manganese oxide in Fig. 1b shows the simi-

lar diffraction peaks as the silica template with the peak position slightly shifted to higher angle. An almost unchanged lattice spacing of $a = 21.2$ nm suggests that the manganese oxide product has inherited the ordered structure of the template. The wide-angle XRD pattern of the manganese oxide in Fig. 1c shows that all of the diffraction peaks of the m-MnO_x sample can be indexed to tetragonal MnO_2 (JCPDS no. 24-0735) and cubic Mn_2O_3 (JCPDS no. 78-0390). According to the quantitative determination of mineral composition by XRD [31], the percentage of tetragonal MnO_2 was calculated based on the normalized ratios of relative intensities for (1 0 1) peak of tetragonal MnO_2 to that for (2 2 2) peak of cubic Mn_2O_3, i.e.:

$$W_{MnO_2} = \frac{I_{MnO_2}}{I_{MnO_2} + I_{Mn_2O_3}(K_{MnO_2}/K_{Mn_2O_3})} \quad (1)$$

W_{MnO_2}, $I_{MnO_2(1\,0\,1)}$ and $I_{Mn_2O_3(2\,2\,2)}$ denote the mass percentage of MnO_2 phase, the relative intensity of (1 0 1) peak for MnO_2 phase and the relative intensity of (2 2 2) peak for cubic Mn_2O_3 phase, respectively. The values of K_{MnO_2} and $K_{Mn_2O_3}$ are 2.7 and 5.05, respectively according to JCPDS 24-0735 and JCPDS 78-0390. Then the calculated mass fraction of MnO_2 phase in the as-prepared sample is 69%. Both of the MnO_2 and Mn_2O_3 phases have been reported with excellent catalytic activity [17,20]. The as-prepared m-MnO_x sample containing the two phases may also exhibit excellent catalytic activity on dye degradation. The EDS analysis in Fig. 1d confirmed the complete removal of silica in the m-MnO_x sample by the silica-etching process.

The N_2 sorption curves of the sample in Fig. 2 show that the as-prepared m-MnO_x sample has a weak jump at $P/P_0 = 0.3$–0.5 corresponding to the capillary condensation of the mesopores produced by the removal of silica wall and another jump at $P/P_0 = 0.8$–0.9 which is typical for mesoporous solids. This indicates that the as-prepared m-MnO_x sample retains the mesoporous structure of the template. The bimodal pore distribution in the range of 2–4 nm and 8–20 nm for the m-MnO_x sample can be seen in the inset of Fig. 2. The pores of 2–4 nm are produced by the removal of silica wall, and those of 8–20 nm may be due to the textural porosity among the particles. For comparison, the N_2 sorption curve of manganese oxide prepared without using silica template was also measured, and the curve is at a much lower position. The BET specific surface areas are 8.44 and 73.3 $m^2\,g^{-1}$ for nm-MnO_x and m-MnO_x samples, respectively, which indicates that the particles may grow much larger without confinement by the framework of the mesoporous silica template.

The representative SEM images of the prepared m-MnO_x sample were shown in Fig. 3a and b. It can be seen that such a material exhibits a flake-like morphology with the dimension of about 80–200 nm. Typical TEM images of the m-MnO_x sample were shown in Fig. 3c and d, which revealed clearly the aligned nanorods and mesoporous structure of the as-prepared m-MnO_x sample. It can be estimated from the TEM image that the diameter of the nanorods for the m-MnO_x sample is about 8 nm. The pore diameter from the TEM images is about 2 nm which is in good agreement with the value obtained from the N_2 sorption (inset of Fig. 2).

3.2. Catalytic property for dye oxidation

To study the catalytic property of the as-prepared m-MnO_x sample, the experiments of RhB degradation were carried out. Various experimental parameters which influenced the decolorization efficiency were investigated under 30–100 °C, such as the catalyst concentration, the pH value of the reaction system and the reaction time.

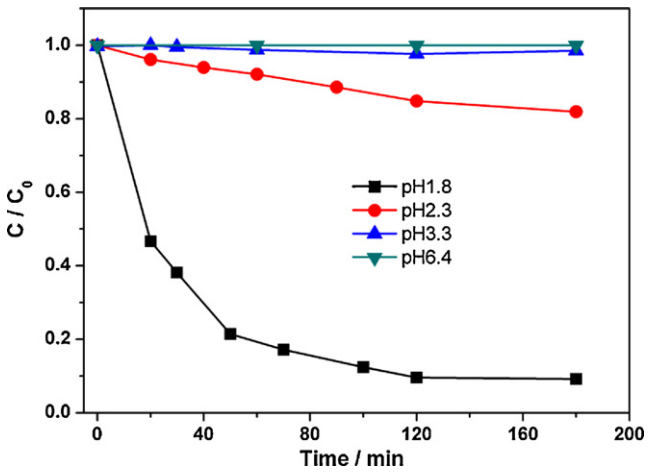

Fig. 5. The decolorization efficiencies of RhB (10^{-4} M) as a function of reaction time under different pH values (catalyst concentration, 0.4 g/L; temperature, 30 °C).

3.2.1. Effect of catalyst concentration

The cost of catalyst was the primary factor contributing to the chemical costs of catalytic oxidation treatment. It was important to minimize the required amount of catalyst. Then investigations of the m-MnO_x concentration on the degradation of RhB dye were conducted. As shown in Fig. 4, the concentration of m-MnO_x had an important influence on the degradation of RhB dye. The RhB degradation efficiency was increased greatly by increasing the m-MnO_x concentration from 0.1 to 0.4 g/L. When the catalyst concentration was higher than 0.4 g/L, the rate of decolorization remains almost constant with the catalyst concentration further increased. This can be explained on the basis that optimum catalyst loading is dependent on initial solute concentration. If the catalyst concentration was increased, the total active surface was increased correspondingly and the enhanced catalytic performance was obtained. However, the increased concentration of catalyst would have no effect on promoting the decolorization efficiency after a maximum catalyst dosage was imposed. This may be ascribed to the increased aggregation of catalyst with a high concentration. Therefore the catalyst concentration of 0.4 g/L was fixed for RhB degradation for further studies.

3.2.2. Effect of pH on the catalytic property

It is important to study the role of pH on decolorization of dye since dye effluents are discharged at different pH. To study the effect

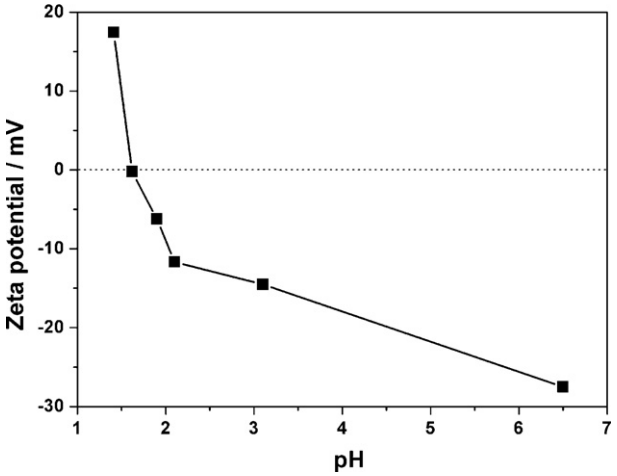

Fig. 6. Zeta potentials of RhB/m-MnO_x suspension under different pH.

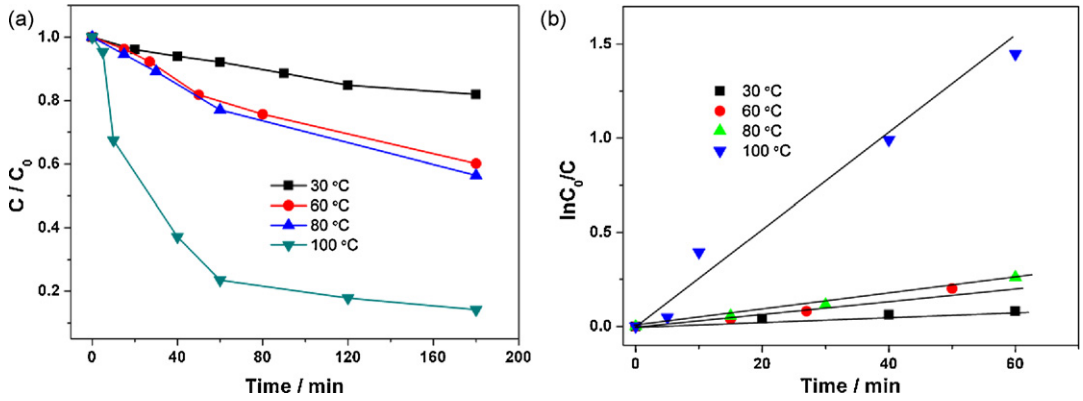

Fig. 7. (a) The decolorization efficiencies of RhB (10^{-4} M) as a function of reaction time under different temperature (catalyst concentration 0.4 g/L, pH 2.3). (b) Kinetic linear simulation curve of RhB (10^{-4} M) catalytic degradation with m-MnO_x under different temperature (catalyst concentration 0.4 g/L, pH 2.3).

of pH on the decolorization efficiency, experiments were carried out at various pH values. Fig. 5 shows the degradation of RhB as a function of reaction time under different pH values. It was found that the decolorization of the RhB dye on m-MnO_x sample was highly pH dependent and increased with decreasing pH. The maximum decolorization efficiency of RhB was 91% at pH 1.8. When the pH value was 6.4, the decolorization of the dye was negligible. The observed pH dependence may be ascribed to the pH effect on the catalyst. It has been reported that the oxidation of organic compounds on manganese oxide involving the diffusion of organic compound to the particle surface to form a complex first, followed by exchange of electrons with reactive surface of manganese (III/IV) oxides [32]. In the catalytic oxidation process, H^+ can enhance the surface acidity of m-MnO_x and make the basic RhB molecules more prone to interact with m-MnO_x. On the other hand, H^+ was required for the detachment of the reaction product Mn(II) from the particle surface so as to expose the underlying reactive Mn(III/IV) sites [33]. These effects lead to the observed increase in decolorization efficiencies with decreasing pH. Both of the MnO_2 and Mn_2O_3 species in the m-MnO_x sample contributed to the oxidation process. It has been reported the flux of Mn(III) and Mn(IV) from the surface into overlying solution is negligible considering that the extremely low solubility of oxides formed from these oxidation states [34].

The zeta potentials of m-MnO_x suspensions under different pH values shown in Fig. 6 further proved the above explanation on the pH dependent catalytic performance. The measured zero point of charge (PZC) for the m-MnO_x sample is at pH 1.6. It has been reported that catalyst exhibits its highest activity near the zero point of charge [35,36]. From this view point, it is easy to understand why the as-prepared sample exhibited much higher oxidation ability at pH 1.8 which is the most proximal pH value to the pH_{zpc} of the m-MnO_x sample in the present experiments.

3.2.3. *Effect of temperature on the catalytic property*

The effect of temperature on the degradation efficiency was studied by varying the temperature in the range of 30–100 °C. Fig. 7a demonstrates the effect of the solution temperature on the degradation of RhB. As expected, the temperature of reaction solution was one of the important effect factors. The degradation efficiencies changed with the variation of temperatures. As shown in Fig. 7a, at 100 °C, the degradation efficiency of RhB dye on the m-MnO_x sample is much higher than that at 30–80 °C. Fig. 7a also indicates the influence of temperature on the decolorization of the dye is relatively insignificant at the initial reaction stage and in a lower temperature range. This may be ascribed to the change of interaction of dye with the particle surface from the fast physisorption to surface chemical reaction at a higher temperature [14]. Fig. 7b shows the kinetics of degradation of RhB on the as-prepared m-MnO_x sample under different reaction temperatures on the basis of the data plotted in Fig. 7a within the first 60 min. The results show that the catalytic degradation of RhB dye in m-MnO_x suspension can be described by the first order kinetic model, $\ln(C_0/C) = kt$, where C_0 is the initial concentration and C is the concentration at time t. The plots with time t as abscissa and $\ln(C_0/C)$ as vertical ordinate are close to linear curves (Fig. 7b). The rate constants k at 30 °C, 60 °C, 80 °C and 100 °C were calculated to be 0.0011 min^{-1}, 0.0037 min^{-1}, 0.0044 min^{-1} and 0.0259 min^{-1}, respectively, indicating a preferable catalytic performance at higher temperature.

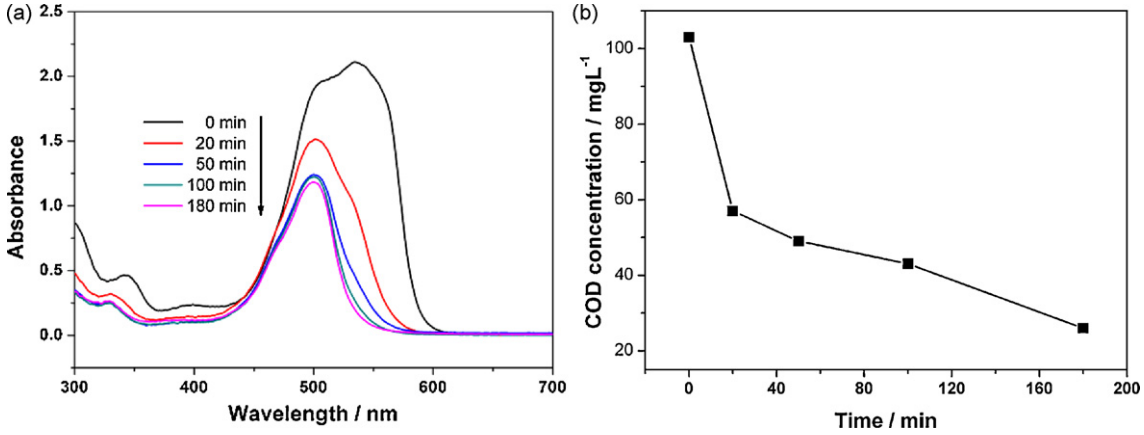

Fig. 8. (a) UV–visible spectral changes of RhB aqueous solution as a function of reaction time. (b) Variation of COD of RhB (10^{-4} M) aqueous solutions with catalytic reaction time (catalyst concentration 0.4 g/L, pH 1.8, temperature 30 °C).

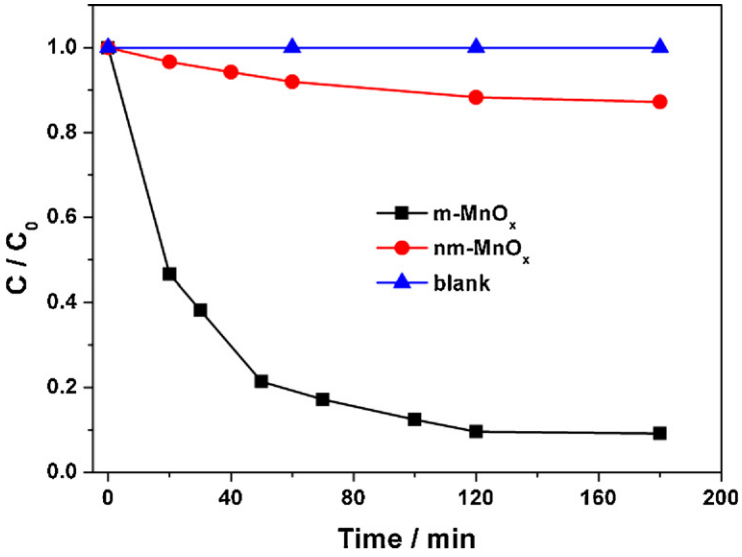

Fig. 9. The decolorization efficiencies of RhB (10^{-4} M) as a function of reaction time by different catalysts (catalyst concentration 0.4 g/L, pH 1.8, temperature 30 °C) and without catalyst (blank).

3.2.4. UV–visible spectral changes of RhB and the related COD reduction

COD value is related to the total concentration of organics in the solution and the decrease of COD reflects the extent of degradation or mineralization of an organic species. The changes in UV–visible spectrum and COD were studied for RhB degradation (initial concentration 10^{-4} mol/L, catalysts concentration 0.4 g/L, pH 1.8, temperature 30 °C) as a function of reaction time.

Fig. 8a displays the temporal evolution of the spectral changes during the degradation of RhB. A rapid decrease of RhB absorption at wavelength of 553 nm was observed, along with an absorption band shifts to shorter wavelengths. This hypsochromic shifts are caused by N-demethylation of RhB [37]. The sharp decrease and shift of the major absorption band within 20 min was along with the obvious decrease of the COD value. As shown in Fig. 8b, the initial COD value of the RhB solution (10^{-4} mol/L) was 103 mg/L. When the catalytic reaction was started, the COD value decreased from 103 to 57 mg/L rapidly within the initial 20 min. After the initial 20 min, the decrease of COD became slower which was similar with the changes of the UV–visible spectrum. Although there was little change in the UV–visible spectrum after 50 min (Fig. 8a), the COD value was further decreased to 26 mg/L when the catalytic reaction time was up to 180 min. This indicated that some colorless intermediates may form in the catalytic process. The reduction in COD confirms the mineralization of RhB along with decolorization.

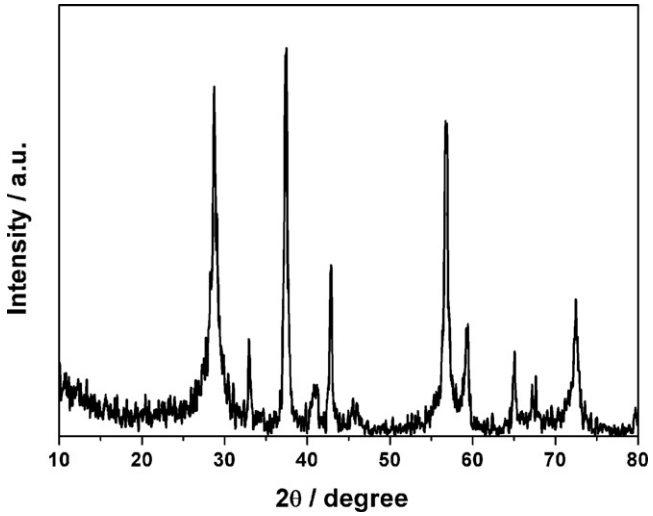

Fig. 10. XRD pattern of the nm-MnO_x sample.

3.2.5. Comparative study

For comparison, the degradation efficiencies of RhB mediated by nm-MnO_x sample as well as without catalyst (blank experiment) were also conducted. As shown in Fig. 9, the degradation of RhB is not observed without any catalyst. However, with the nm-MnO_x sample as a catalyst, about 13% of the RhB is decolorized after 180 min. If the m-MnO_x sample was used under the same conditions, about 91% of the RhB was decolorized at the same time (as mentioned above), indicating the obvious advantage of mesoporous material in the RhB decolorization. The chemical composition of the nm-MnO_x sample was detected by XRD, as shown in Fig. 10. Similar to the m-MnO_x sample, the nm-MnO_x sample was also composed of tetragonal MnO_2 (JCPDS no. 24-0735) and cubic Mn_2O_3 (JCPDS no. 78-0390). A difference is the Mn_2O_3 phase in the nm-MnO_x sample was much less than that in the m-MnO_x sample. Both of the surface area and the chemical composition may contribute to the different catalytic performance.

4. Conclusion

Ordered mesoporous manganese oxide which consists of catalytic active MnO_2 and Mn_2O_3 phases has been successfully synthesized by a simple template casting method. Compared with the nm-MnO_x sample, the as-prepared m-MnO_x sample exhibited much enhanced catalytic activity in RhB oxidation. The catalytic performance of the m-MnO_x sample was found greatly influenced by the catalyst concentration, the reaction temperature and the pH value of the reaction system. The optimum catalyst concentration was 0.4 g/L for the degradation of 10^{-4} mol/L RhB solution. With the increasing of the reaction temperature or the decreasing of pH values, the catalytic performance was much enhanced. Besides the color removal, the decrease in COD of the RhB solution was also observed indicating the mineralization of the RhB dye in the catalytic oxidation process. It can be concluded that the m-MnO_x assisted catalytic degradation of textile dyes may be an economic, environmentally benign and efficient treatment.

Acknowledgements

We acknowledge the financial support from the National Natural Science Foundation of China (50732004), National Basic Research Program of China (2007CB613305, 2010CB933503) and the Nanotechnology Programs of Science and Technology Commission of Shanghai (0852nm00500, 0952nm00400).

References

[1] T. Sriskandakumar, N. Opembe, C.-H. Chen, A. Morey, C. Kingondu, S.L. Suib, J. Phys. Chem. A 113 (2009) 1523.
[2] T.F. Robinson, G. McMullan, R. Marchant, P. Nigam, Bioresour. Technol. 77 (2001) 247.
[3] P.P. Zamora, A. Kunz, S.G. Moraes, R. Pelegrini, P.C. Moleiro, J. Reyes, N. Duran, Chemosphere 38 (1999) 835.
[4] L. Ladakowicz, M. Solecka, R. Zylla, J. Biotechnol. 89 (2001) 175.
[5] D. Georgiou, P. Melidis, A. Aivasidis, K. Gimouhopoulos, Dyes Pigments 52 (2002) 69.
[6] I. Arslan, I.A. Balcioglu, T. Tuhkanen, D. Bahnemann, J. Environ. Eng. 126 (2000) 903.
[7] S.K. Chaudhuri, B. Sur, J. Environ. Eng. 126 (2000) 583.
[8] N. Stock, J. Peller, K. Vinodgopal, P.V. Kamat, Environ. Sci. Technol. 34 (2000) 1747.
[9] I.M. Banat, P. Nigam, D. Singh, R. Marchant, Bioresour. Technol. 58 (1996) 217.
[10] C.L. Hsueh, Y.H. Huang, C.C. Wang, C.Y. Chen, Chemosphere 58 (2005) 1409.
[11] H. Lachheb, E. Puzenat, A. Houas, M. Ksibi, E. Elaloui, C. Guillard, J.-M. Herrmann, Appl. Catal. B 39 (2002) 75.
[12] C.A. Martınez-Huitle, E. Brillas, Appl. Catal. B 87 (2009) 105.
[13] A.H. Gemeay, R.G. El-Sharkawy, I.A. Mansour, A.B. Zaki, Appl. Catal. B 80 (2008) 106.
[14] R. Liu, H. Tang, Water Res. 34 (2000) 4029.
[15] W. Zhang, Z. Yang, X. Wang, Y. Zhang, X. Wen, S. Yang, Catal. Commun. 7 (2006) 408.
[16] R. Radhakrishnan, S.T. Oyama, J.G. Chen, K. Asakura, J. Phys. Chem. B 105 (2001) 4245.
[17] Y. Dong, H. Yang, K. He, S. Song, A. Zhang, Appl. Catal. B 85 (2009) 155.
[18] M.A. Hasan, M.I. Zaki, L. Pasupulety, K. Kumari, Appl. Catal. A 181 (1999) 171.
[19] L. Espinal, S.L. Suib, J.F. Rusling, J. Am. Chem. Soc. 126 (2004) 7676.
[20] Y.-F. Han, F. Chen, Z. Zhong, K. Ramesh, L. Chen, E. Widjaja, J. Phys. Chem. B 110 (2006) 24450.
[21] S. Liang, F. Teng, G. Bulgan, R. Zong, Y. Zhu, J. Phys. Chem. C 112 (2008) 5307.
[22] G. Marbán, T. Valdés-Solís, A.B. Fuertes, J. Catal. 226 (2004) 138.
[23] M. Casapu, O. Krocher, M. Elsener, Appl. Catal. B 88 (2009) 413.
[24] B. Jiang, Y. Liu, Z. Wu, J. Hazard. Mater. 162 (2009) 1249.
[25] L.M. Gandía, M.A. Vicente, A. Gil, Appl. Catal. B 38 (2002) 295.
[26] D. Delimaris, T. Ioannides, Appl. Catal. B 84 (2008) 303.
[27] Q. Tang, X. Huang, Y. Chen, T. Liu, Y. Yang, J. Mol. Catal. A: Chem. 301 (2009) 24.
[28] A.T. Bell, Science 299 (2003) 1688.
[29] J.G. Yu, J.F. Xiong, B. Cheng, S.W. Liu, Appl. Catal. B 60 (2005) 211.
[30] F. Kleitz, S.H. Choi, R. Ryoo, Chem. Commun. 17 (2003) 2136.
[31] G.A. Pawloski, US Patent 4,592,082 (1986).
[32] A.T. Stone, Environ. Sci. Technol. 21 (1987) 979.
[33] J. Klausen, S.B. Haderlein, R.P. Schwarzenbach, Environ. Sci. Technol. 31 (1997) 2642.
[34] A.T. Stone, J.J. Morgan, Environ. Sci. Technol. 18 (1984) 450.
[35] A. Mokhtar, Y.L. Nargess, M.M. Niyaz, S.T. Nooshin, J. Hazard. Mater. 135 (2006) 171.
[36] D. Chen, A.K. Ray, Water Res. 32 (1998) 3223.
[37] W. Zhao, C. Chen, X. Li, J. Zhao, J. Phys. Chem. B 106 (2002) 5022.